Title:

Maintaining Single-Channel Recordings on a Silver Nanoneedle Through Probe Design and Feedback Tip Positioning Control

Essraa A. Hussein[§] and Ryan J. White[*§‡]*

[§] Department of Chemistry, University of Cincinnati, Cincinnati, OH 45221

[‡] Department of Electrical Engineering and Computer Science, University of Cincinnati, Cincinnati, OH 45221

Corresponding Author Email: ryan.white@uc.edu

Abstract:

Ion channel proteins showed great promise in the field of nanopore sensing and molecular flux imaging applications due to the atomic-level precision of the pore size and high signal-to-noise ratio. More specifically, ion channel probes, where the protein channels are integrated at the end of a solid probe, can achieve highly localized detection. Metal probe materials such as gold and silver have been developed to support lipid bilayers and enable the use of smaller probes, or nanoneedles, compared to more traditional glass micropipette ion channel probes. Silver probes are preferable because they support sustained DC stable channel current due to the AgCl layer formed around the tip during the fabrication process. However, one of the current challenges in ion channel measurements is maintaining a single-channel recording. Multiple protein insertions complicate data analysis and destabilize the bilayer. Herein, we combine the promising probe material (Ag/AgCl) with an approach based on current feedback controlled tip-positioning to maintain long-term single-channel recordings up to 3 hours. We develop a hybrid positioning control system, where the channel current is used as feedback to control the vertical movement of the silver tip and subsequently, control the number of protein channels inserted in the lipid membrane. Our findings reveal that the area of lipid bilayer decreases with moving the silver tip up (i.e., decreasing the displacement in the z-direction). By reducing the bilayer area around the fine silver tip, we minimize the probability of multiple insertions and remove unwanted proteins. In addition, we characterize the effect of lipid properties such as fluidity on the lipid membrane area. We believe that the use of silver nanoneedle, which enables DC stable channel current, coupled with the developed tip displacement mechanism will offer more opportunities to employ these probes for chemical imaging and mapping different surfaces.

Introduction

Ion channel proteins are an integral part of many cellular membranes and play key roles in regulating the permeability of cell membranes, especially in heart, nerve, and muscle cells.[1–4] In addition, ion channels also serve as a target for many drug discoveries to study the interaction between the ion channel and the active pharmaceutical component and monitor the protein-ligand activity.[5] Inspired by nature, researchers harnessed the ability to monitor the passage of the ions through the channels and have employed these measurements for the development of sensing tools for diverse applications. The diversity of techniques include nanopore sensing, DNA sequencing, and chemical imaging with ion channels.[6–10] When the ion channels are embedded in a membrane insulating two electrolyte baths, these protein channels provide the sole path for ions when applying a potential across the membrane. Driven by the applied potential, the ions move freely between the two electrolyte sides- the ions movement is recognized by a quantized current step, also known as open channel current. Small molecules or analytes that exist in the electrolyte bath can pass through or bind to the ion channel, leading to a temporary blockade of ions movement, identified by downward current events or resistive pulses. Characterization of these binding events enables the identification and quantification of the target analyte by analyzing the event time and amplitude, and events frequency, respectively.[11–13]

Ion channel measurements have been an attractive means to detect small molecules or biomarkers,[14–16] monitor molecular flux,[17,18] sequence DNA or RNA,[19–21] and study the kinetic activity of proteins and peptides[22,23] due to high sensitivity, inherent signal amplification, and robust sensor structure.[1,6–8] However, the sensing capabilities of these measurements are still limited by some challenges. One of the major challenges is the ability to maintain a single protein channel throughout the recording time. Although increasing the number of ion channels would increase the frequency of binding events, and accordingly enhance the sensitivity, multiple insertions also leads to a complicated current signal used to determine analyte concentration.[24] This signal complexity stems from the possibility of simultaneous events, which means more than a single binding event occurs synchronously from more than one protein channel. In detail, when multiple protein channels are inserted in the lipid membrane, the likelihood of simultaneous binding events rises, rendering the analysis of the events characteristics more difficult.[24] Additionally, multiple protein insertions destabilize the lipid membrane and may result in bilayer rupture.[25]

There are many methods reported in the literature to obtain single channel recordings.[26–34] For example using a microfluidic chip, where the excess protein was perfused n after single protein channel insertion to prevent additional insertions.[31] Michele *et al.*[30] utilized a polymeric device to form lipid bilayers and a proteo-liposome to deliver a single channel into the formed bilayer. However, the aforementioned methods either involve complicated steps or require the fabrication of microdevices. Other methods rely on the use of a glass microtip to transfer ion channels from a bacterial colony to a planner lipid membrane.[28] Similarly, Holden and Bayley engaged a solid probe from an agarose gel dome containing protein channels into a bilayer chamber until a single ion channel is identified.[26] In another approach, Hall and co-workers used a DNA-tethered α-hemolysin protein pore to capture a single channel at a solid-state nanopore, where the DNA molecule was threaded through when the potential was applied, pulling the protein pore until it's stopped at the synthetic nanopore opening.[33] Chemically, Bayley and co-workers used amphiphiles to prevent further protein insertions without interruption of bilayer stability.[35] More recently, an electronic microsystem was developed for single ion channel detection, where a complementary metal–oxide–semiconductor (CMOS) instrumentation was designed to detect a single ion channel event.[34] Unfortunately, the reported methods failed to handle the case of multiple protein insertions and some of them suffer from a very low yield of single channel insertions.[34] Furthermore, none of the reported methods stated long-term single channel recordings i.e., on the hours time-scale.

We recently developed a silver nanoneedle ion channel probe that manifested a great ability to obtain a sustained, DC stable channel current, attributed to the formation of AgCl layer around the silver tip.[36] Herein, we combine the promising probe material (Ag/AgCl)[36,37] with an approach based on tip-positioning control to maintain single-channel recordings. We develop a hybrid positioning control system, where we can prevent multiple protein insertions and remove unwanted proteins. In this approach, the channel current is used as feedback to control the vertical movement of the silver tip so that we can control the number of protein channels inserted in the lipid membrane. Our findings demonstrate the feasibility of the proposed approach to maintain long-term single channel recordings (up to 3 hrs). In addition, we found that the area of lipid bilayer decreases with moving the silver tip up (i.e., decreasing the displacement in the z-direction). Based on these results, we hypothesize that by reducing the bilayer area around the fine silver tip, we can minimize the probability of multiple insertions and remove unwanted proteins. In addition, we characterize the effect of different lipids on the lipid membrane area and properties. This will provide more precise control over lipid membrane and protein insertion, and thus, we can maintain long-term single-channel recordings suitable for future imaging applications.

Methods

Chemicals and Reagents

For Silver nanoneedle fabrication, we used a silver microwire (250 μm diameter) of 99.99% purity (Alfa Aesar), perchloric acid (70% $HClO_4$; Sigma-Aldrich), and methanol (HPLC grade; Sigma-Aldrich). O-(3-carboxypropyl)-O′-[2-(3-mercaptopropionylamino)ethyl] propyl ethylene glycol (MW 3000; Sigma-Aldrich) or thiol PEG was used as ethanolic solution (ethanol proof, Decon Laboratories, Inc., PA) for surface modification. An electrolyte/buffer solution was made of potassium chloride (KCl; Sigma-Aldrich) or potassium nitrate (KNO_3; Sigma-Aldrich) in a sodium phosphate buffer (pH 7.4) composed of sodium dihydrogen phosphate ($NaH_2PO_4 \cdot 2H_2O$; Sigma-Aldrich) and disodium phosphate (Na_2HPO_4, Sigma-Aldrich). The buffer solution was prepared using ultrapure water from a Milli-Q (Merck Millipore Corp.) resisted 18.2 MΩ at 25 °C. Three different phospholipids were used to prepare the oil/lipid mixture and form the lipid bilayer; 1,2-dipalmitoyl-sn-glycero-3-phosphocholine (DPPC), 1,2-Diphytanoyl-sn-glycero-3-phosphocholine (DPhPC), 1,2-dioleoyl-sn-glycero-3-phosphocholine (DOPC), and 1,2-dilinolenoyl-sn-glycero-3-phosphocholine (DLPC)- all lipids were purchased from Avanti Polar Lipids and mixed with n-decane (Merck Millipore Corp.). Alpha-hemolysin (αHL; Sigma-Aldrich) isolated from *Staphylococcus aureus* was used as a monomer protein powder. Single strand DNA (ssDNA, poly dA50; Integrated DNA T) was used as the target analyte for single-molecule detection.

Fabrication of silver nanoneedle and formation of the lipid bilayer

Silver nanoneedle was fabricated by electrochemical etching of a 250 μm silver wire using perchloric acid solution as recently described in detail.[36] Briefly, the 1-2 mm end of a silver microwire was etched in a perchloric acid: methanol solution (1:4, respectively) with applying a DC voltage of 1V. The etching process was complete when the current dropped to zero and a cone-shaped tip was formed. The etched silver tip was then rinsed thoroughly and modified with Thiol PEG (MW 3000), which supports an aqueous electrolyte layer around the tip to be ready for measurements.[36] The method of lipid bilayer formation was previously mentioned.[36,38–40] More specifically, we followed the detailed method we recently published,[36] where the silver probe is inserted into a chamber with two compartments: oil/lipid phase (10 mg/mL of DPhPC, DOPC, or DLP solution in n-decane) at the top and an aqueous buffered electrolyte bath solution of 2M KCl underneath the lipid compartment. With the first vertical movement of the silver probe down to the chamber and retracting it again, we formed the first lipid monolayer around the tip at the oil/air

interface, then, with the second movement, the monolayer around the tip combined with the monolayer at the oil/water interface.

Single channel recordings

After the formation of lipid bilayer, the αHL protein channels were reconstituted in the lipid membrane. Protein insertion was recognized by monitoring the ionic current. We developed an approach, where the protein channel current is used as feedback to control the vertical movement of silver tip. In detail, by moving the silver nanoneedle probe down along the z-axis, multiple protein insertion was observed and vice versa. By controlling such a vertical tip movement, we can control the number of proteins inserted in the lipid membrane and thus, maintain single channel recordings. Figure SI.1 shows the proposed three folded approach, where we basically control tip displacement by monitoring the channel current, enhance the bilayer stability by lowering the applied potential across the membrane, and tune the protein concentration to enable maintaining single channel recordings and prevent multiple insertions. All measurements were performed on an optical table and within a Faraday cage to reduce low frequency electronic ambient noise.

Membrane capacitance measurement and calculation of membrane area

To investigate why the number of proteins inserted in lipid membrane increases with moving the silver probe down, we calculate the lipid bilayer area at different z positions and then, calculate the membrane area using equation (1).[41–44]

$$C_{mem} = \frac{\varepsilon_{\circ}\, \varepsilon\, A}{d} \qquad (1)$$

In equation (1), C_{mem} is the lipid membrane capacitance measured at different z positions using Pico2 Tecella amplifier, $\boldsymbol{\varepsilon}_{\circ}$ is the permittivity of free space ($\varepsilon_{\circ}$ = 8.854 x10^{14} F cm^{-1}), $\boldsymbol{\varepsilon}$ is the dielectric constant of the lipid bilayer (ε ~ 2.1), $\boldsymbol{d}$ is the thickness of bilayer, which is estimated to be 4nm [45–49] and $\boldsymbol{A}$ denotes to the surface area of the lipid membrane. We used equation (1) to calculate the surface area of different types of bilayers composed of lipids with different fluidities such as DPhPC, DOPC, and DLPC bilayers. The structures of these phospholipids are provided in Figure S2, the lipid fluidity increase by increasing the degree of lipid unsaturation.[50–54]

Instrumentation and data analyses

Ion channel recordings were collected using a Degan Chem-Clamp low-noise potentiostat (Minneapolis, MN) coupled to a PC using an in-house written LabVIEW program (National

Instruments, Austin, TX). Controlling the probe displacement was achieved by a z-axis piezo actuator (PI (Physik Instruments) L.P., Auburn, MA) and a Multi-Micromanipulator Systems (MPC-200 controller and ROE). A patch-clamp amplifier (PICO 2, Tecella) with a 7.9 kHz low-pass filter at a sampling frequency of 40kHz was used to measure the membrane capacitance. In all experiments, the silver nanoneedle probe acted as a working electrode (WE), while another Ag/AgCl wire inserted in the bath solution was used as a Quasi reference electrode (QRE). Data analyses including creating current time traces, current vs z-displacement plot, and bilayer area vs z-displacement were obtained using MATLAB R2019b, Python 3.9.7, and OriginPro 2017.

Results and Discussion

We recently reported the feasibility of silver nanoneedle to support DC stable ion channel recordings and mitigate the problem of channel current decay shown in other metal nanoneedles such as gold.[36,40,55] The stable current behavior of silver nanoneedle is attributed to the AgCl layer formed around the silver tip during the etching process rendering the tip acts eventually as Ag/AgCl, non-polarizable electrode .[36,37] However, there are some existing challenges such as the ability to control protein insertions and maintain long-term single-channel recordings in an intact lipid membrane. To address these challenges, herein, we develop an approach where we can control the number of proteins inserted in the lipid bilayer by controlling the tip positioning along the z-axis with respect to the oil: water interface, besides tuning protein concentration, and increasing the stability of lipid membrane by lowering the potential applied across the membrane (see Figure S1 and Figure 1). We applied this approach to maintain single channel recordings for more than 3 hours and prevent multiple protein insertions. We hypothesize that controlling the vertical movement of silver probe provide more control over the lipid bilayer area and thus, the number of proteins inserted in the bilayer. Accordingly, we quantitatively characterized the effect of the tip z-displacement on the obtained bilayer area. In addition, we varied the lipid membrane composition by using phospholipids of different fluidities and investigated the effect of the different lipids on the membrane area.

Formation of the lipid membrane and channel current recordings

We used the silver nanoneedle fabricated by electrochemical etching in perchloric acid to form a AgCl layer at the silver surface and modified with thiol-PEG (MW 3000) to support an aqueous electrolyte layer around the silver tip, as recently reported.[36] When the silver nanoneedle was pushed down to the oil/lipid aqueous interface, the lipid bilayer was formed via tip-dip method and supported at the silver tip similar to previous reports.[36,38–40,55] The formation of lipid bilayer was confirmed by measuring the membrane capacitance, where an increment of ~5-10 pF is

sufficient to indicate that the bilayer was successfully formed at the probe tip. Additionally, quantized current steps were observed, indicating insertion of αHL protein. There are some other measures in the literature to verify the successful formation of bilayer such as continuously monitoring the ionic current until it drops to zero or applying a high potential (~1V) to electrically break the lipid membrane. However, measuring the membrane capacitance is a more convenient and quantitative measure for lipid bilayer formation since helps to monitor the bilayer formation at the molecular level, and correlates the capacitance with the bilayer area.[17,47,56–58] After the bilayer formation, αHL protein insertion was recognized by step-like current steps, each current step is quantized and indicates single protein inserted in the lipid membrane as indicated in Figure S3. This current increase is attributed to ions free movement through the protein channel. The channel current observed while using silver nanoneedle as an ion channel probe is stable over time, compared to gold probes with similar geometries.[40,55]

Feedback-controlled tip displacement mechanism for long-term single channel measurements

In order to control the number of protein channels and maintain single channel recordings for prolonged time, we developed an approach where the channel current is used as feedback to control the silver tip movement. In our proposed approach, we use a hybrid positioning system to control the z-displacement of silver tip. Figure 2 demonstrates the general principle of the proposed approach. First, we use an automated positioning system using the z-piezo actuator to move the silver probe down across the oil/lipid aqueous interface, this movement enables the bilayer formation as well as protein insertion. However, the z-piezo vertical movement is programmed to stop at a current threshold equivalent to single open channel current value (~100 pA). After single protein insertion, we perform a "precautionary retraction" using the z-stepper motor to prevent additional protein insertions and allow maintaining a single channel. The precautionary retraction was typically executed very slowly and to a distance ranging from 60 μm to 140 μm. Furthermore, if a second protein is inserted in the bilayer (which will be recognized by a second current step), we perform a "controlled de-insertion", which is another vertical movement to de-insert the second protein from the lipid membrane. Although the tip positioning control resulted in removing additional proteins (see Figure 2), we can't determine which protein molecule was de-inserted and which was maintained (original or second inserted protein) since the αHL heptameric ion channels have the same conductance in the same experimental conditions.[59,60] Thus, we use the open channel current, which is quantized, as feedback to obtain single channel recordings, prevent multiple insertions, and remove unwanted proteins. We applied this feedback-

controlled mechanism to αHL protein channel in 2M KCl with applying a potential of 50 mV and we successfully obtained long-term single channel recordings ranging from 25 minutes to 3 hours17-minute-long single open channel measurements as illustrated in Figure 3. In contrast to other reported techniques to maintain single channel recordings,[27,29,31,32,61,62] our proposed approach can weed out the unwanted proteins and allow for performing spatially resolved measurements. In addition, this approach doesn't require any specific fabricated devices or involve any complicated steps.

Detection of ssDNA

To demonstrate the feasibility of our approach for nanopore sensing, we applied the proposed approach to achieve long-term, single molecule detection of poly dA 50 ssDNA. Since ssDNA molecules can translocate through αHL channel from both channel sides, we performed the detection experiment with bath-side configuration, where the protein molecules and ssDNA molecules are in the bath chamber. To enhance the capture rate and slow down the translocation rate of the negatively charged DNA molecules, we applied asymmetric salt concentration and decreased the applied potential to 50 mV, respectively.[19,63–65] Figure 4 shows the binding events of ssDNA when it passes through αHL pore, blocking the ions flow through the protein. We demonstrate the ability of the proposed approach to control protein insertion via tip-positioning to prevent multiple protein insertions and maintain single channel recordings, with a stable and sustained open channel current for 25 min (Figure 4) and up to 2 hours as shown in Figure S4. We statistically compare the open channel current with and without target molecules- Figure S5 demonstrates the distribution of channel current in the presence and absence of the target analyte, ssDNA. These results demonstrate the applicability of our approach to maintain single channel along with the silver probe architecture to be able to obtain sustained and stable ion channel recordings suitable for future analytical applications.

Correlation between silver probe z-displacement and bilayer area

We hypothesize that regulating the vertical movement of the silver probe affects the lipid membrane area. In other words, when we move the tip down, the bilayer area increases, offering more chances for multiple protein insertions. In contrast, moving the probe up decreases the surface are of the bilayer, and with tuning protein concentration, will minimize the probability of multiple insertions and help to remove any additional unwanted proteins from the membrane. In order to test this hypothesis, we quantitatively characterize the effect of the tip z-displacement on the bilayer area. To achieve this, we measure the lipid membrane capacitance (C_{mem}), which is

then correlated to the membrane area according to equation (1). We record C_{mem} values at different z-positions by moving the probe up and down along a z-distance of 300 μm. Then, we calculate the bilayer area respective to C_{mem} values at each z-position using equation (1). Figure 5 shows that as the z-displacement increases (i.e., moving the probe down), the lipid bilayer area increases accordingly and vice versa. We demonstrate the vertical movement either up or down shows a similar trend, in other words, moving down or increasing z-displacements results in higher membrane capacitance and thus, larger bilayer area. Similarly, moving the probe up or decreasing the z-displacement results in decreased membrane capacitance and accordingly, lower bilayer area. Although it might be expected that the change in bilayer area would happen when moving the silver probe at a sub-micrometer scale, the results showed that the appreciable bilayer area change has occurred with micrometer scale tip displacement. These findings are consistent with our previous report, which also required μm-scale movement to analyze the protein de-insertion current.[55]

To understand the way that bilayer area changes with the vertical movement of the silver probe, we initially assumed that the bilayer may be conformed around the silver tip, forming a cone-shape, identical to the silver tip shape. By using the formula in Figure S6 and given the probe dimensions (specifically the cone angle, measured from SEM micrographs and averaged for six probes as shown in Figure S7), we calculated the lateral surface area of a cone at different (h) equivalent to different z-displacement (see page S4). We expected to see a cone area close to the bilayer area shown before in Figure 5. However, when the lateral surface area of a cone was fit with the calculated bilayer area, we found that the calculated cone area is significantly higher than the found bilayer area (see Figure S8). Based on these findings, we then assumed that the lipid bilayer is not completely conformed around the tip and doesn't match up the cone shape.

The effect of varying lipid fluidity on the membrane surface area

To further investigate our assumption about the way the bilayer is formed around the silver tip, we studied how the bilayer properties, such as fluidity, can affect the bilayer shape and area. Bilayer fluidity is a function of different parameters such as fatty acid chain length, fatty acid saturation degree, temperature, and charge.[66] In this study, we varied the bilayer fluidity by varying the unsaturation degree of the hydrocarbon fatty acid tails in the phospholipids. The arrangement of the fatty acid hydrocarbon interior of the lipid bilayer plays a key role in the formed bilayer area; saturated fatty acid tails with linear arrangement of hydrocarbons results in tight packing of lipid molecules. While the kinks in the double bonds of the unsaturated fatty acids

disorder the packing of the hydrocarbon chain, leading to more fluid structures.[50–52,67] We used three different phospholipids: saturated phospholipid (DPhPC), unsaturated with two double bonds (DOPC), and unsaturated with six double bonds (DLPC), see Figure S2. After the lipid bilayers were successfully formed using the three phospholipids, the C_{mem} for each one was recorded, and the corresponding membrane surface area was calculated using equation (1) at different Z-displacements. Figure 6 shows the correlation between bilayer area formed using the different phospholipids and Z-positions of the silver tip. These results show that the higher degree of fatty acid unsaturation, the higher bilayer fluidity, and the larger lateral surface area, in agreement with previous reports in literature.[48,50,67] The kinked tails of unsaturated fatty acid occupy a larger lateral surface area when packed within the bilayers compared to a straight lipid tail of saturated fatty acids.[50,67] It's noteworthy to mention that we tried to use the rigid, fully saturated lipid without methyl groups, DPPC, but we couldn't record membrane capacitance for this lipid with moving the silver probe down.

In addition to the effect of fluidity on the obtained bilayer surface area, we believe this effect is extended to the bilayer mechanical properties such as deformability, which could affect the bilayer shape as well.[68–70] According to previous reports that studied the deformation of lipid membranes, we assume that the vertical movement of the silver tip would apply some force or physical pressure on the bilayer, where the higher the fluidity, the more deformable membrane.[68–73] However, we believe that further detailed studies are required to quantitatively investigate the effect of a solid probe pushing the lipid bilayer with the vertical displacement of the probe.

Conclusion

In this paper, we introduce a combination between an optimized ion channel probe, silver nanoneedle, and a mechanism to obtain long-term single channel recordings. The probe design of silver nanoneedle enables a sustained, DC stable open channel current, when compared to other probes with similar geometries, such as gold. In addition, we report a tip-positioning mechanism, where we use the channel current as feedback to control protein insertion and maintain single channel recordings for more than 3 hours. We correlate the tip-positioning mechanism with the lipid membrane area- our findings reveal that the area of lipid bilayer decreases with moving the silver tip up (i.e., decreasing the displacement in the z-direction). Finally, we studied the effect of lipid bilayer composition and the corresponding membrane area. We believe that silver nanoneedle, coupled with the developed tip displacement mechanism will offer more opportunities to employ these probes for different analytical applications.

Supporting information

Purposed approach to maintain long-term single channel recordings, phospholipid structures, current-time traces for protein insertion and bilayer rupture, single molecule detection of ssDNA, histogram for open channel current, surface area of a cone, cone angle measurement, and lipid bilayer area in comparison with the cone lateral surface area.

Acknowledgments

This work was supported by the National Science Foundation (CHE 1608679 and CHE 2108368).

References

(1) Varongchayakul, N.; Song, J.; Meller, A.; Grinstaff, M. W. Single-Molecule Protein Sensing in a Nanopore: A Tutorial. *Chem. Soc. Rev.* **2018**, *47*, 8512–8524. https://doi.org/10.1039/c8cs00106e.

(2) Kratz, J. M.; Grienke, U.; Scheel, O.; Mann, S. A.; Rollinger, J. M. Natural Products Modulating the HERG Channel: Heartaches and Hope. *Nat. Prod. Rep.* **2017**, *34*, 957–980. https://doi.org/10.1039/C7NP00014F.

(3) Chui, J. K. W.; Fyles, T. M. Ionic Conductance of Synthetic Channels: Analysis{,} Lessons{,} and Recommendations. *Chem. Soc. Rev.* **2012**, *41*, 148–175. https://doi.org/10.1039/C1CS15099E.

(4) Aramesh, M.; Forró, C.; Dorwling-Carter, L.; Lüchtefeld, I.; Schlotter, T.; Ihle, S. J.; Shorubalko, I.; Hosseini, V.; Momotenko, D.; Zambelli, T.; et al. Localized Detection of Ions and Biomolecules with a Force-Controlled Scanning Nanopore Microscope. *Nat. Nanotechnol.* **2019**, *14*, 791–798. https://doi.org/10.1038/s41565-019-0493-z.

(5) Paul J. England. Drug_Discovery_and_Introduction-Diary. *Drug Discov. Today* **1999**, *4* (9), 391–392.

(6) Lazenby, R. A.; Macazo, F. C.; Wormsbecher, R. F.; White, R. J. Quantitative Framework for Stochastic Nanopore Sensors Using Multiple Channels. *Anal. Chem.* **2018**, *90*, 903–911. https://doi.org/10.1021/acs.analchem.7b03845.

(7) Cao, C.; Long, Y. T. Biological Nanopores: Confined Spaces for Electrochemical Single-Molecule Analysis. *Acc. Chem. Res.* **2018**, *51*, 331–341. https://doi.org/10.1021/acs.accounts.7b00143.

(8) Shi, W.; Friedman, A. K.; Baker, L. A. Nanopore Sensing. *Anal. Chem.* **2017**, *89*, 157–188. https://doi.org/10.1021/acs.analchem.6b04260.

(9) Wu, Y.; Tilley, R. D.; Gooding, J. J. Challenges and Solutions in Developing Ultrasensitive Biosensors. *J. Am. Chem. Soc.* **2019**, *141*, 1162–1170. https://doi.org/10.1021/jacs.8b09397.

(10) Robertson, J. W. F.; Ghimire, M. L.; Reiner, J. E. Nanopore Sensing: A Physical-Chemical Approach. *Biochim. Biophys. Acta - Biomembr.* **2021**, *1863*, 183644. https://doi.org/10.1016/j.bbamem.2021.183644.

(11) Bayley, H.; Martin, C. R. Resistive-Pulse Sensing - from Microbes to Molecules. *Chem. Rev.* **2000**, *100*, 2575–2594. https://doi.org/10.1021/cr980099g.

(12) Kozak, D.; Anderson, W.; Vogel, R.; Trau, M. Advances in Resistive Pulse Sensors: Devices Bridging the Void between Molecular and Microscopic Detection. *Nano Today* **2011**, *6*, 531–545. https://doi.org/10.1016/j.nantod.2011.08.012.

(13) Pan, R.; Hu, K.; Jiang, D.; Samuni, U.; Mirkin, M. V. Electrochemical Resistive-Pulse Sensing. *J. Am. Chem. Soc.* **2020**, *141*, 19555–19559. https://doi.org/10.1021/jacs.9b10329.

(14) Yang, L.; Yamamoto, T. Quantification of Virus Particles Using Nanopore-Based Resistive-Pulse Sensing Techniques. *Front. Microbiol.* **2016**, *7*, 1–7. https://doi.org/10.3389/fmicb.2016.01500.

(15) Hiratani, M.; Kawano, R. DNA Logic Operation with Nanopore Decoding to Recognize MicroRNA Patterns in Small Cell Lung Cancer. *Anal. Chem.* **2018**, *90*, 8531–8537. https://doi.org/10.1021/acs.analchem.8b01586.

(16) Liu, P.; Kawano, R. Recognition of Single-Point Mutation Using a Biological Nanopore. *Small Methods* **2020**, *4*, 1–7. https://doi.org/10.1002/smtd.202000101.

(17) Macazo, F. C.; White, R. J. Bioinspired Protein Channel-Based Scanning Ion Conductance Microscopy (Bio-SICM) for Simultaneous Conductance and Specific Molecular Imaging. *J. Am. Chem. Soc.* **2016**, *138*, 2793–2801. https://doi.org/10.1021/jacs.5b13252.

(18) Shi, W.; Zeng, Y.; Zhu, C.; Xiao, Y.; Cummins, T. R.; Hou, J.; Baker, L. A. Characterization of Membrane Patch-Ion Channel Probes for Scanning Ion Conductance Microscopy. *Small* **2018**, *14*, 1–10. https://doi.org/10.1002/smll.201702945.

(19) Branton, D.; Deamer, D. W.; Marziali, A.; Bayley, H.; Benner, S. A.; Butler, T.; Ventra, M. Di; Garaj, S.; Hibbs, A.; Huang, X.; et al. The Potential and Challenges of Nanopore Sequencing. *Nanosci. Technol.* **2008**, *26*, 261–268. https://doi.org/10.1142/9789814287005_0027.

(20) Clarke, J.; Wu, H. C.; Jayasinghe, L.; Patel, A.; Reid, S.; Bayley, H. Continuous Base Identification for Single-Molecule Nanopore DNA Sequencing. *Nat. Nanotechnol.* **2009**, *4*, 265–270. https://doi.org/10.1038/nnano.2009.12.

(21) Venkatesan, B. M.; Bashir, R. Nanopore Sensors for Nucleic Acid Analysis. *Nat. Nanotechnol.* **2011**, *6*, 615–624. https://doi.org/10.1038/nnano.2011.129.

(22) Zhao, Q.; De Zoysa, R. S. S.; Wang, D.; Jayawardhana, D. A.; Guan, X. Real-Time Monitoring of Peptide Cleavage Using a Nanopore Probe. *J. Am. Chem. Soc.* **2009**, *131*, 6324–6325. https://doi.org/10.1021/ja9004893.

(23) Macrae, M. X.; Blake, S.; Jiang, X.; Capone, R.; Estes, D. J.; Mayer, M.; Yang, J. A Semi-Synthetic Ion Channel Platform for Detection of Phosphatase and Protease Activity. *ACS Nano* **2009**, *3*, 3567–3580. https://doi.org/10.1021/nn901231h.

(24) Ervin, E. N.; White, R. J.; White, H. S. Sensitivity and Signal Complexity as a Function of the Number of Ion Channels in a Stochastic Sensor. *Anal. Chem.* **2009**, *81*, 533–537. https://doi.org/10.1021/ac801104v.

(25) van Uitert, I.; Le Gac, S.; van den Berg, A. The Influence of Different Membrane Components on the Electrical Stability of Bilayer Lipid Membranes. *Biochim. Biophys. Acta - Biomembr.* **2010**, *1798*, 21–31. https://doi.org/https://doi.org/10.1016/j.bbamem.2009.10.003.

(26) Holden, M. A.; Bayley, H. Direct Introduction of Single Protein Channels and Pores into Lipid Bilayers. *J. Am. Chem. Soc.* **2005**, *127*, 6502–6503. https://doi.org/10.1021/ja042470p.

(27) Uni, V.; Ox, O.; Kingdom, U.; Holden, M. A.; Bayley, H. Direct Introduction of Single Protein Channels and Pores into Lipid Bilayers. *J. Am. Chem. Soc.* **2005**, *127*, 6502–6503.

(28) Holden, M. A.; Jayasinghe, L.; Daltrop, O.; Mason, A.; Bayley, H. Direct Transfer of Membrane Proteins from Bacteria to Planar Bilayers for Rapid Screening by Single-Channel Recording. *Nat. Chem. Biol.* **2006**, *2*, 314–318. https://doi.org/10.1038/nchembio793.

(29) Holden, M. A.; Jayasinghe, L.; Daltrop, O.; Mason, A.; Bayley, H. Direct Transfer of Membrane Proteins from Bacteria to Planar Bilayers for Rapid Screening by Single-Channel Recording. *Nat. Chem. Biol.* **2006**, *2*, 314–318. https://doi.org/10.1038/nchembio793.

(30) Zagnoni, M.; Sandison, M. E.; Marius, P.; Lee, A. G.; Morgan, H. Controlled Delivery of

Proteins into Bilayer Lipid Membranes on Chip. *Lab Chip* **2007**, *7*, 1176–1183. https://doi.org/10.1039/B703818F.

(31) Shim, J. W.; Gu, L. Q. Stochastic Sensing on a Modular Chip Containing a Single-Ion Channel. *Anal. Chem.* **2007**, *79*, 2207–2213. https://doi.org/10.1021/ac0614285.

(32) Kang, X.; Cheley, S.; Rice-ficht, A. C.; Bayley, H. A Storable Encapsulated Bilayer Chip Containing a Single Protein Nanopore. *J. Am. Chem. Soc.* **2007**, *129*, 4701–4705.

(33) Hall, A. R.; Scott, A.; Rotem, D.; Mehta, K. K.; Bayley, H.; Dekker, C. Hybrid Pore Formation by Directed Insertion of α-Haemolysin into Solid-State Nanopores. *Nat. Nanotechnol.* **2010**, *5*, 874–877. https://doi.org/10.1038/nnano.2010.237.

(34) Liu, X.; Li, L.; Mason, A. J. High Throughput Single-Ion-Channel Array Microsystem with CMOS Instrumentation. *IEEE* **2014**, *2014*, 2765–2768. https://doi.org/10.1109/EMBC.2014.6944196.

(35) Raychaudhuri, P.; Li, Q.; Mason, A.; Mikhailova, E.; Heron, A. J.; Bayley, H. Fluorinated Amphiphiles Control the Insertion of α-Hemolysin Pores into Lipid Bilayers. *Biochemistry* **2011**, *50*, 1599–1606. https://doi.org/10.1021/bi1012386.

(36) Hussein, E. A.; White, R. J. Silver Nanoneedle Probes Enable Sustained DC Current, Single-Channel Resistive Pulse Nanopore Sensing. *Anal. Chem.* **2021**, *93*, 11568–11575. https://doi.org/10.1021/acs.analchem.1c02087.

(37) Shoji, K.; Kawano, R.; White, R. J. Recessed Ag/AgCl Microelectrode-Supported Lipid Bilayer for Nanopore Sensing. *Anal. Chem.* **2020**, *92*, 10856–10862. https://doi.org/10.1021/acs.analchem.0c02720.

(38) Okuno, D.; Hirano, M.; Yokota, H.; Ichinose, J.; Kira, T.; Hijiya, T.; Uozumi, C.; Yamakami, M.; Ide, T. A Gold Nano-Electrode for Single Ion Channel Recordings. *Nanoscale* **2018**, *10*, 4036–4040. https://doi.org/10.1039/c7nr08098k.

(39) Okuno, D.; Hirano, M.; Yokota, H.; Onishi, Y.; Ichinose, J.; Ide, T. A Simple Method for Ion Channel Recordings Using Fine Gold Electrode. *Anal. Sci.* **2016**, *32*, 1353–1357. https://doi.org/10.2116/analsci.32.1353.

(40) Shoji, K.; Kawano, R.; White, R. J. Spatially Resolved Chemical Detection with a Nanoneedle-Probe-Supported Biological Nanopore. *ACS Nano* **2019**, *13*, 2606–2614. https://doi.org/10.1021/acsnano.8b09667.

(41) Alagappan, M.; Kandaswamy, A.; Kumaravel, M.; Rameshkumar, S. Interaction of Cholesterol with Artificial Bilayer Lipid Membrane System and Development of an Electrochemical Sensor. *Arab. J. Chem.* **2020**, *13*, 423–430. https://doi.org/10.1016/j.arabjc.2017.05.013.

(42) Steinem, C.; Janshoff, A.; Ulrich, W. P.; Sieber, M.; Galla, H. J. Impedance Analysis of Supported Lipid Bilayer Membranes: A Scrutiny of Different Preparation Techniques. *Biochim. Biophys. Acta - Biomembr.* **1996**, *1279*, 169–180. https://doi.org/10.1016/0005-2736(95)00274-X.

(43) Gentet, L. J.; Stuart, G. J.; Clements, J. D. Direct Measurement of Specific Membrane Capacitance in Neurons. *Biophys. J.* **2000**, *79*, 314–320. https://doi.org/10.1016/S0006-3495(00)76293-X.

(44) Heimburg, T. The Capacitance and Electromechanical Coupling of Lipid Membranes Close to Transitions: The Effect of Electrostriction. *Biophys. J.* **2012**, *103*, 918–929. https://doi.org/10.1016/j.bpj.2012.07.010.

(45) Moellerfeld, J.; Prass, W.; Ringsdorf, H.; Hamazaki, H.; Sunamoto, J. Improved Stability of Black Lipid Membranes by Coating with Polysaccharide Derivatives Bearing Hydrophobic Anchor Groups. *BBA - Biomembr.* **1986**, *857*, 265–270. https://doi.org/10.1016/0005-2736(86)90355-X.

(46) Minamikawa, H.; Hato, M. Phase Behavior of Synthetic Phytanyl-Chained Glycolipid/Water Systems. *Langmuir* **1997**, *13*, 2564–2571. https://doi.org/10.1021/la961037t.

(47) Hirano-Iwata, A.; Niwano, M.; Sugawara, M. The Design of Molecular Sensing Interfaces with Lipid-Bilayer Assemblies. *TrAC - Trends Anal. Chem.* **2008**, *27*, 512–520. https://doi.org/10.1016/j.trac.2008.04.006.

(48) Enterohemorrhagic, F. A.; Erhardt, M.; Petra, C. The Impact of Plasma Membrane Lipid Composition on Flagellum-Mediated Adhesion of Enterohemorrhagic Escherichia Col. *msphere* **2020**, *5*, 702–720.

(49) Ermilova, I.; Swenson, J. DOPC: Versus DOPE as a Helper Lipid for Gene-Therapies: Molecular Dynamics Simulations with DLin-MC3-DMA. *Phys. Chem. Chem. Phys.* **2020**, *22*, 28256–28268. https://doi.org/10.1039/d0cp05111j.

(50) Sukit, L.; Cho, H. J; Wu, Y.; Wright, N. T.; Sum, A. K.; Chan, C.; The Role of Fatty Acid Unsaturation in Minimizing Biophysical Changes on the Structure and Local Effects of Bilayer Membranes. *Biochim. Biophys. Acta* **2009**, *1788*, 1508–1516. https://doi.org/10.1016/j.bbamem.2009.04.002.The.

(51) Yang, X.; Sheng, W.; Sun, G. Y.; Lee, J. Effects of Fatty Acid Unsaturation Numbers on Membrane Fluidity and α-Secretase-Dependent Amyloid Precursor Protein Processing. *Gerontology* **2015**, *61*, 515–525. https://doi.org/10.1016/j.neuint.2010.12.004.Effects.

(52) Reglinski, K.; Steinfort-Effelsberg, L.; Sezgin, E.; Klose, C.; Platta, H. W.; Girzalsky, W.; Eggeling, C.; Erdmann, R. Fluidity and Lipid Composition of Membranes of Peroxisomes, Mitochondria and the ER From Oleic Acid-Induced Saccharomyces Cerevisiae. *Front. Cell Dev. Biol.* **2020**, *8*, 1–12. https://doi.org/10.3389/fcell.2020.574363.

(53) Nagle, J. F.; Jablin, M. S.; Tristram-Nagle, S.; Akabori, K. What Are the True Values of the Bending Modulus of Simple Lipid Bilayers? *Chem. Phys. Lipids* **2015**, *185*, 3–10. https://doi.org/10.1016/j.chemphyslip.2014.04.003.

(54) Rokitskaya, T. I.; Kotova, E. A.; Agapov, I. I.; Moisenovich, M. M.; Antonenko, Y. N. Unsaturated Lipids Protect the Integral Membrane Peptide Gramicidin A from Singlet Oxygen. *FEBS Lett.* **2014**, *588*, 1590–1595. https://doi.org/10.1016/j.febslet.2014.02.046.

(55) Shoji, K.; Kawano, R.; White, R. J. Analysis of Membrane Protein Deinsertion-Associated Currents with Nanoneedle-Supported Bilayers to Discover Pore Formation Mechanisms. *Langmuir* **2020**, *36*, 10012–10021. https://doi.org/10.1021/acs.langmuir.0c00833.

(56) Funakoshi, K.; Suzuki, H.; Takeuchi, S. Lipid Bilayer Formation by Contacting Monolayers in a Microfluidic Device for Membrane Protein Analysis. *Anal. Chem.* **2006**, *78*, 8169–8174. https://doi.org/10.1021/ac0613479.

(57) Gross, L. C. M.; Heron, A. J.; Baca, S. C.; Wallace, M. I. Determining Membrane Capacitance by Dynamic Control of Droplet Interface Bilayer Area. *Langmuir* **2011**, *27*, 14335–14342. https://doi.org/10.1021/la203081v.

(58) Heitz, B. A.; Xu, J.; Jones, I. W.; Keogh, J. P.; Comi, T. J.; Hall, H. K.; Aspinwall, C. A.; Saavedra, S. S. Polymerized Planar Suspended Lipid Bilayers for Single Ion Channel Recordings : Comparison of Several Dienoyl Lipids. *Langmuir* **2011**, *27*, 1882–1890. https://doi.org/10.1021/la1025944.

(59) Maglia, G.; Heron, A. J.; Stoddart, D.; Japrung, D.; Bayley, H. Analysis of Single Nucleic Acid Molecules with Protein Nanopores. In *Methods in Enzymology*; Elsevier Inc., 2010; Vol. 475, pp 591–623. https://doi.org/10.1016/S0076-6879(10)75022-9.

(60) Oukhaled, G.; Bacri, L.; Mathé, J.; Pelta, J.; Auvray, L. Effect of Screening on the Transport of Polyelectrolytes through Nanopores. *Europhys. Lett.* **2008**, *82*, 48003-p1-48003-p5. https://doi.org/10.1209/0295-5075/82/48003.

(61) Raychaudhuri, P.; Li, Q.; Mason, A.; Mikhailova, E.; Heron, A. J.; Bayley, H. Fluorinated Amphiphiles Control the Insertion of R -Hemolysin Pores into Lipid Bilayers. *Biochemistry* **2011**, *50*, 1599–1606. https://doi.org/10.1021/bi1012386.

(62) Hall, A. R.; Scott, A.; Rotem, D.; Mehta, K. K.; Bayley, H.; Dekker, C. Hybrid Pore Formation by Directed Insertion of α-Haemolysin into Solid-State Nanopores. *Nat. Nanotechnol.* **2010**, *5* (12), 874–877. https://doi.org/10.1038/nnano.2010.237.

(63) De Zoysa, R. S. S.; Jayawardhana, D. A.; Zhao, Q.; Wang, D.; Armstrong, D. W.; Guan, X. Slowing DNA Translocation through Nanopores Using a Solution Containing Organic Salts. *J. Phys. Chem. B* **2009**, *113*, 13332–13336. https://doi.org/10.1021/jp9040293.

(64) Meller, A.; Nivon, L.; Branton, D. Voltage-Driven DNA Translocations through a Nanopore. *Phys. Rev. Lett.* **2001**, *86*, 3435–3438. https://doi.org/10.1103/PhysRevLett.86.3435.

(65) Wanunu, M.; Morrison, W.; Rabin, Y.; Grosberg, A. Y.; Meller, A. Electrostatic Focusing of Unlabelled DNA into Nanoscale Pores Using a Salt Gradient. *Nat. Nanotechnol.* **2010**, *5*, 160–165. https://doi.org/10.1038/nnano.2009.379.

(66) Sen, A.; Ghosh, P. K.; Mukherjea, M. Changes in Lipid Composition and Fluidity of Human Placental Basal Membrane and Modulation of Bilayer Protein Functions with Progress of Gestation. *Mol. Cell. Biochem.* **1998**, *187*, 183–190. https://doi.org/10.1023/A:1006839711587.

(67) Venkatesan, G. A.; Taylor, G. J.; Basham, C. M.; Brady, N. G.; Collier, C. P.; Sarles, S. A. Evaporation-Induced Monolayer Compression Improves Droplet Interface Bilayer Formation Using Unsaturated Lipids. *Biomicrofluidics* **2018**, *12*, 024101/13. https://doi.org/10.1063/1.5016523.

(68) Faizi, H. A.; Dimova, R.; Vlahovska, P. M. A Vesicle Microrheometer for High-Throughput

Viscosity Measurements of Lipid and Polymer Membranes. *Biophys. J.* **2022**, *121*, 910–918. https://doi.org/10.1016/j.bpj.2022.02.015.

(69) Dazzoni, R.; Grélard, A.; Morvan, E.; Bouter, A.; Applebee, C. J.; Loquet, A.; Larijani, B.; Dufourc, E. J. The Unprecedented Membrane Deformation of the Human Nuclear Envelope, in a Magnetic Field, Indicates Formation of Nuclear Membrane Invaginations. *Sci. Rep.* **2020**, *10*, 1–14. https://doi.org/10.1038/s41598-020-61746-0.

(70) Youhei, F. Small Deformation of a Liposome in a Linear Shear Flow. *Fluid Dyn. Res.* **1995**, *15*, 1–11. https://doi.org/10.1016/0169-5983(94)00040-7.

(71) Needham, D.; Nunn, R. S. Elastic Deformation and Failure of Lipid Bilayer Membranes Containing Cholesterol. *Biophys. J.* **1990**, *58*, 997–1009. https://doi.org/10.1016/S0006-3495(90)82444-9.

(72) Okuda, S.; Eiraku, M. Role of Molecular Turnover in Dynamic Deformation of a Three-Dimensional Cellular Membrane. *Biomech. Model. Mechanobiol.* **2017**, *16*, 1805–1818. https://doi.org/10.1007/s10237-017-0920-8.

(73) Espinosa, G.; López-Montero, I.; Monroya, F.; Langevin, D. Shear Rheology of Lipid Monolayers and Insights on Membrane Fluidity. *Proc. Natl. Acad. Sci. U. S. A.* **2011**, *108*, 6008–6013. https://doi.org/10.1073/pnas.1018572108.

FIGURES

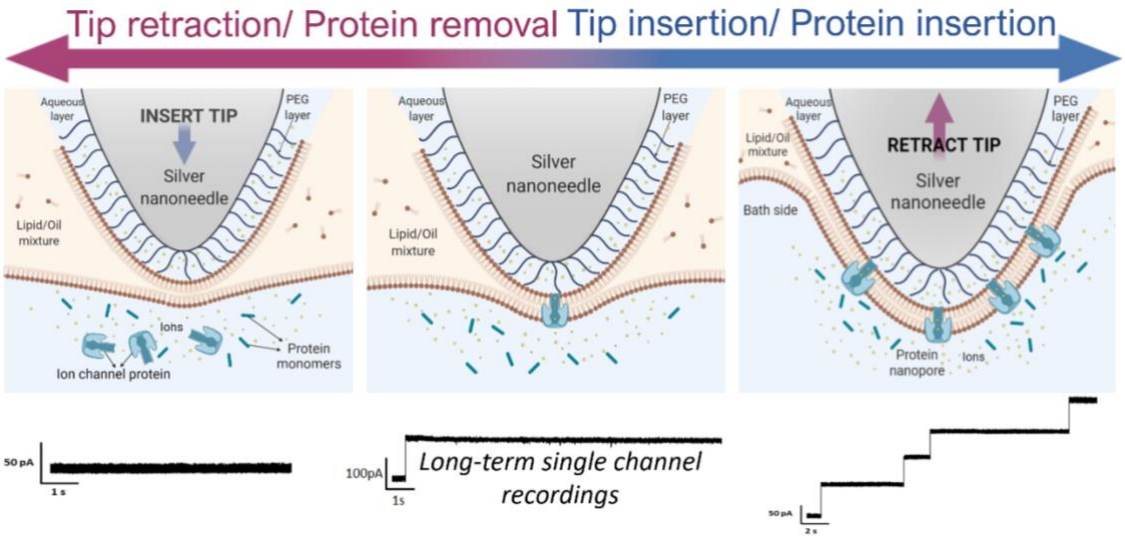

Figure 1. Schematic diagram illustrates the mechanism of controlling protein insertion by controlling the vertical movement of silver nanoneedle with respect to the oil: water interface. Left-to-right direction (Blue arrow): moving the silver probe down, or tip insertion, results in multiple protein insertion in the lipid membrane as indicated by the quantized change in current. Right-to-left direction (Pink arrow): moving the silver probe up, or tip retraction, results in proteins de-insertion from the lipid bilayer. Our approach is based on controlled vertical movement of the probe to achieve more control over the number of proteins inserted in the lipid membrane and maintain single-channel recordings.

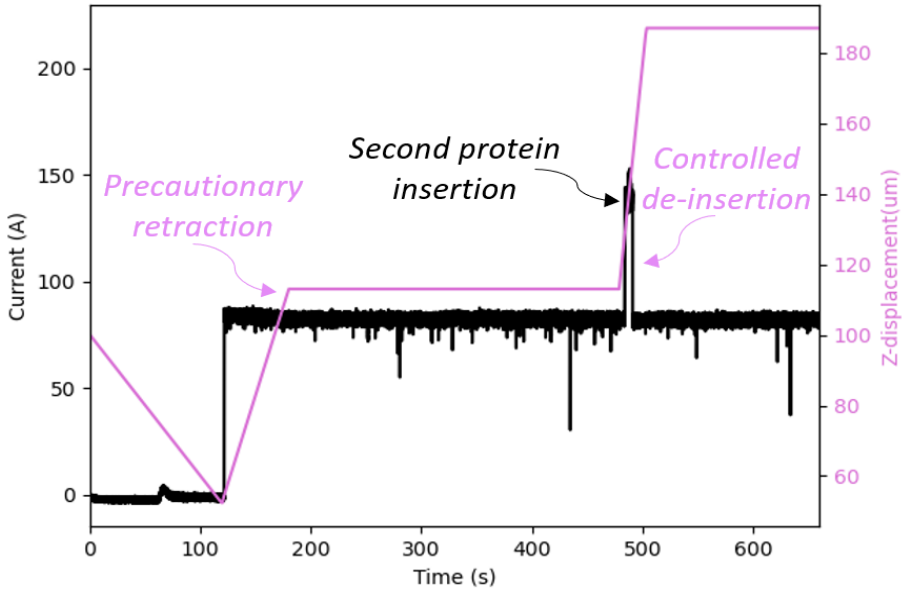

Figure 2. General principle of the current feedback-regulated mechanism to maintain single channel recordings. The black graph represents the current-time traces for αHL open channel current, where each current step indicates a single protein insertion. The pink plot illustrates the vertical displacement of the silver probe (right y-axis) with time. The channel current (left y-axis) is used as feedback to control the probe positioning (right y-axis). Once a second protein is inserted (second current step), we perform a "controlled de-insertion" by moving the silver probe up.

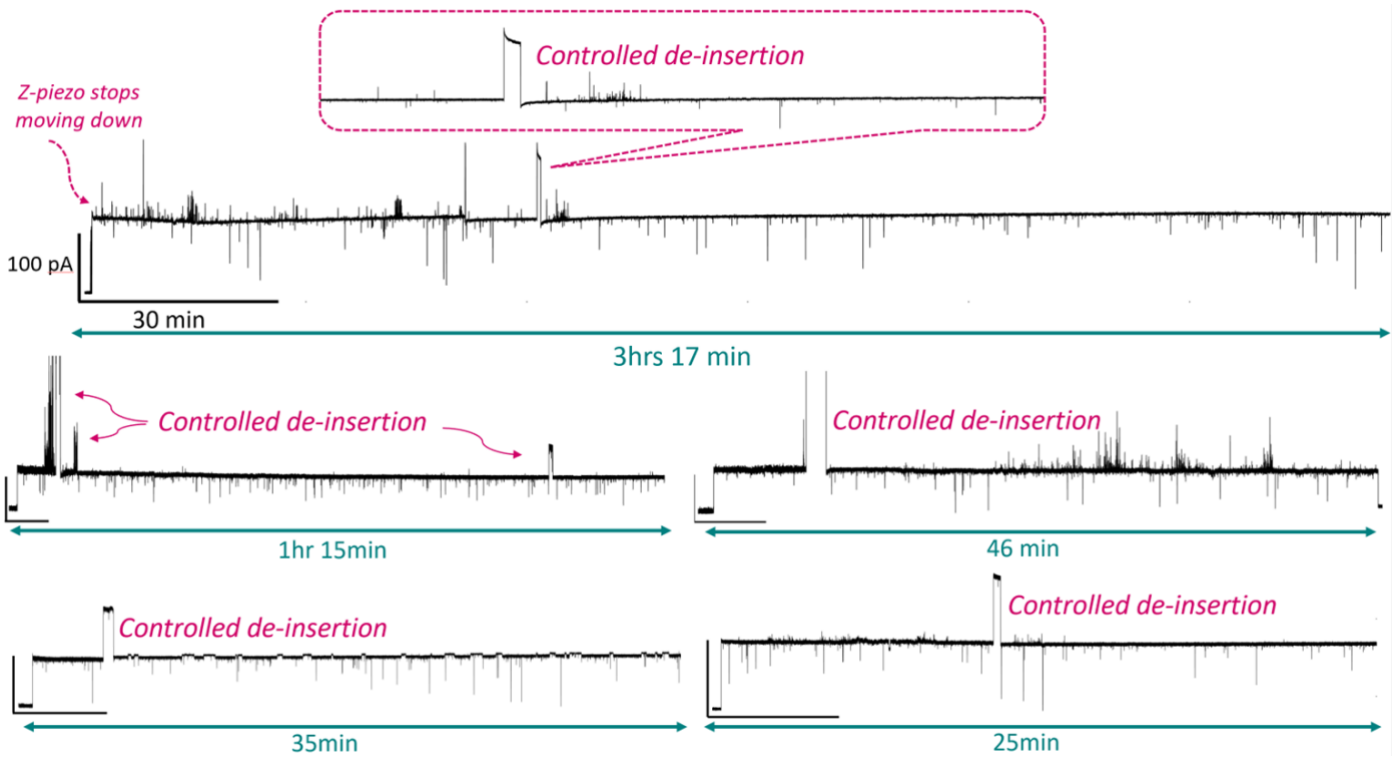

Figure 3. Long-term measurements for αHL open channel current achieved by using silver nanoneedle ion channel probe and applying the proposed approach of a current feedback-controlled z-displacement of the silver probe. The current-time traces show up to more than 3 hours, stable channel current and performing a controlled de-insertion to remove additional protein insertion. All scale bars are 100pA and 5min.

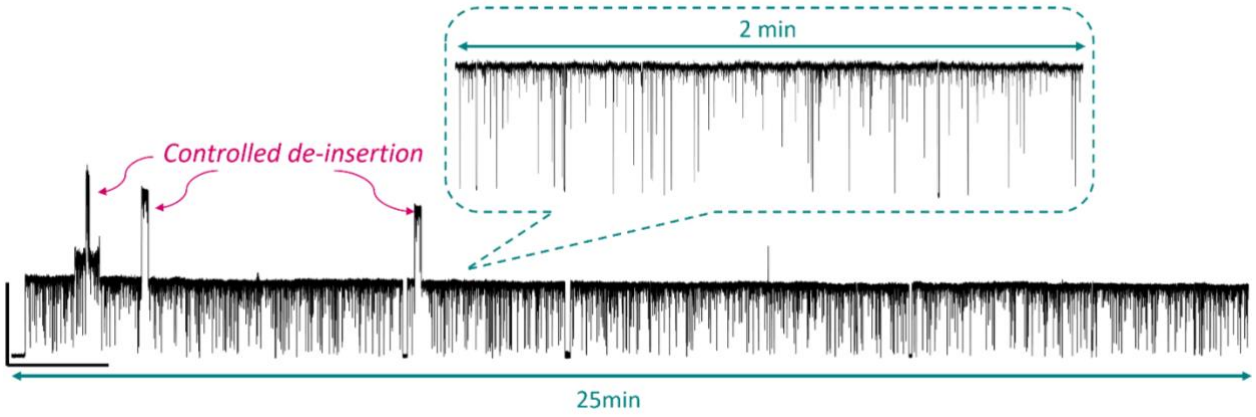

Figure 4. Detection of ssDNA translocation events through single αHL channel supported on the silver nanoneedle probe. The figure demonstrates the ability of the proposed approach to control protein insertion via tip-positioning to maintain single channel throughout the measurement time. The zoomed-in inset shows the binding events of ssDNA molecules.

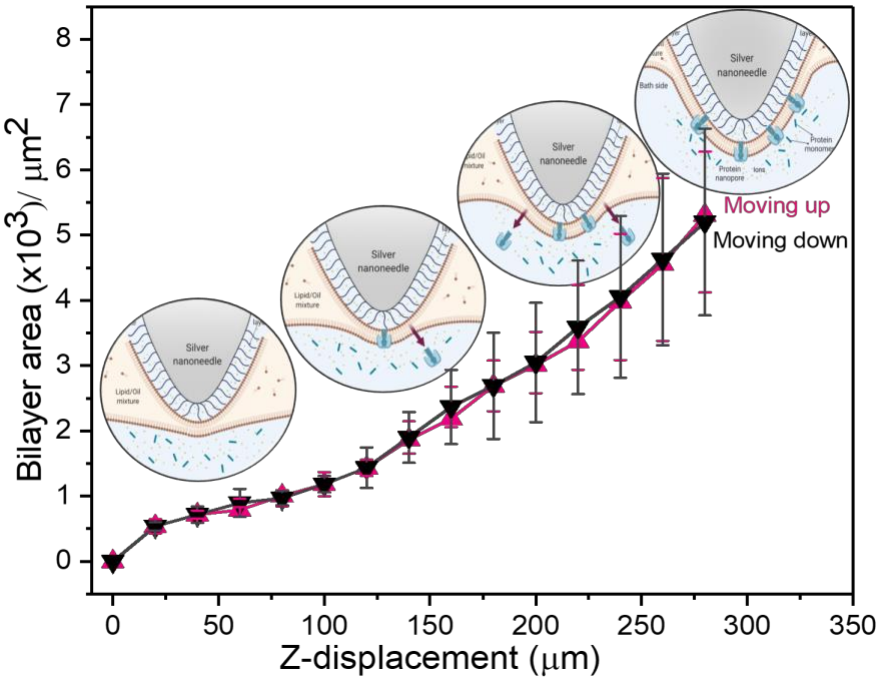

Figure 5. Correlation between the lipid bilayer area and the vertical movement of silver nanoneedle probe. As illustrated in the inset figures, when moving the probe down (or increasing the Z-displacement), the lipid membrane area increases, resulting in multiple protein insertions.

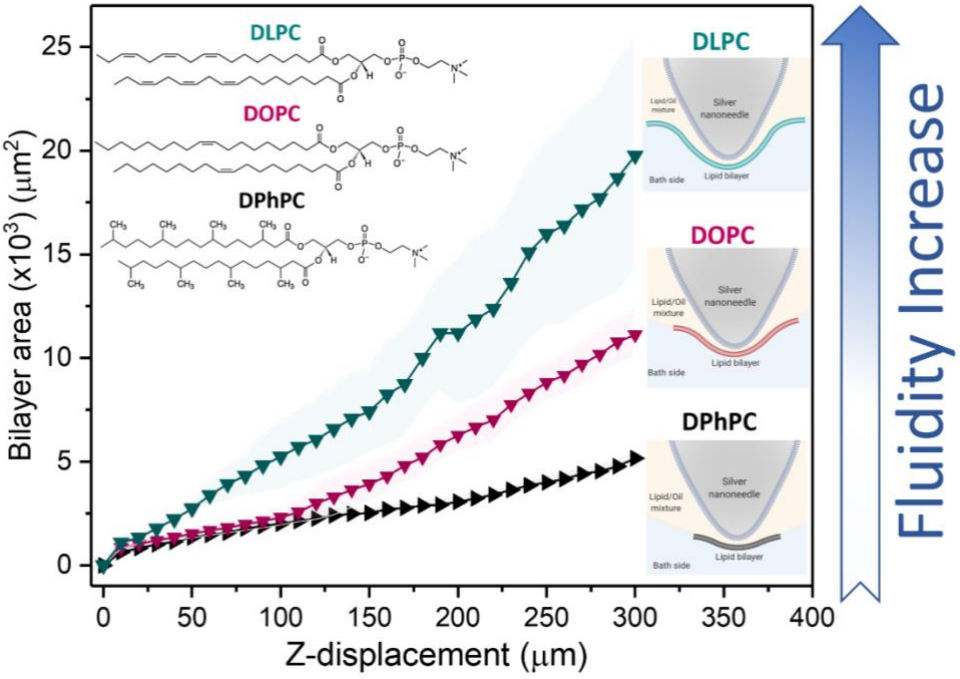

Figure 6. Lipid membrane area vs silver tip displacement for three phospholipids of different fluidity. More fluid lipids resulted in larger surface area for the lipid bilayer formed around the silver nanoneedle tip. Fluidity increases as the degree of unsaturation of phospholipids increases as shown in the chemical structures (top left corner).

TOC Graphic

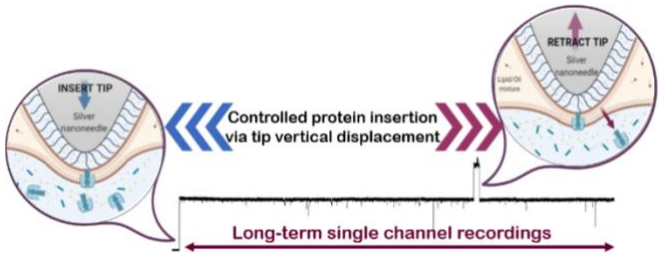
INSERT TIP
Silver nanoneedle
Controlled protein insertion
via tip vertical displacement
RETRACT TIP
Silver nanoneedle
Lipid/Oil mixture
Long-term single channel recordings